original article

Annals of Oncology 19: 1875–1881, 2008
doi:10.1093/annonc/mdn405
Published online 17 July 2008

Telomere shortening is correlated with the DNA damage response and telomeric protein down-regulation in colorectal preneoplastic lesions

C. M. Raynaud[1], S. J. Jang[2], P. Nuciforo[3], S. Lantuejoul[4], E. Brambilla[4], N. Mounier[5], K. A. Olaussen[6], F. André[6], L. Morat[1], L. Sabatier[1] & J.-C. Soria[1,6]*

[1]*Laboratoire de radiobiologie et oncologie, CEA, Fontenay-aux-Roses, France;* [2]*Department of Pathology, Assan Medical Center, Uslan University Medical College, Seoul, South Korea;* [3]*FIRC Institute of Molecular Oncology Foundation, Milan, Italy;* [4]*Department of Pathology CHU A Michallon and INSERM U 823 A Bonniot Institut Grenoble, France;* [5]*Department of Onco-Hematology, Hospital l'Archet, CHU de Nice, Nice, France;* [6]*Division of Cancer Medicine, IGR, Villejuif, France*

Received 26 February 2008; revised 26 May 2008; accepted 28 May 2008

Background: A relation between telomere attrition in early carcinogenesis and activation of DNA damage response (DDR) has been proposed. We explored telomere length and its link with DDR in colorectal multistep carcinogenesis.
Patients and methods: We studied normal mucosa, low-grade dysplasia (LGD) and high-grade dysplasia (HGD) and invasive carcinoma (IC) in matched human colon specimens by evaluating p-ataxia telangiectasia mutated (ATM), p-checkpoint kinase 2 (Chk2), c-H2AX, TRF1 and TRF2 expressions by immunohistochemistry. FISH was used to assess telomere length.
Results: Telomeres shortened significantly from normal (N) to LGD and HGD ($P < 0.0001$; $P = 0.012$), then increased in length in IC ($P = 0.006$). TRF1 and TRF2 expressions were diminished from N to LGD and HGD ($P = 0.004$, $P < 0.0001$, ns) and were reexpressed at the invasive stage ($P = 0.053$ and $P = 0.046$). Phosphorylated ATM, Chk2 and H2AX appeared already in LGD (respectively, $P = 0.001$, $P = 0.002$ and $P = 0.02$). Their expression decreased from HGD to IC (respectively, $P = 0.03$, $P = 0.02$ and $P = 0.37$). These activating phosphorylations were inversely correlated with telomere length and TRF1/2 expression.
Conclusion: In a model of colon multistep carcinogenesis, our data indicate that telomeric length and protein expression levels are inversely correlated with the activation of the DDR pathway.
Key words: Carcinogenesis, DNA damage repair, telomeres, telomeric proteins

introduction

Carcinogenesis is a multistep, multifocal process characterized by the accumulation of genetic and molecular abnormalities. These events generally follow exposure to carcinogens and result in the selection of clonal cells with uncontrolled growth [1]. Cancer develops in a stepwise manner, through a series of events, from preinvasive histological changes to invasive disease [2]. The earliest events are mutations, deletions or polysomy at genomic level, but these changes do not always lead to changes in cell morphology or tissue structure [3, 4]. Current knowledge suggests that the progression of cancer from a premalignant to a malignant state is, consistent with a mechanistic model, based on of the principle of natural selection. Tumor cells acquire the hallmarks of cancer during this carcinogenic selection process [5]. Cell immortality is one of the principal features acquired during this process. Immortality involves the stabilization of telomere length, which is achieved by telomerase activation in ~80% of human tumors.

Correspondence to: Dr J.-C. Soria, Department of Medecine, Institut Gustave Roussy, 39 Rue Camille Desmoulins, 94805 Villejuif, France. Tel: +33-1-42-11-42-91; Fax: +33-1-42-11-52-17; E-mail: soria@igr.fr

Interestingly, telomere length abnormality also appears to be one of the earliest and most prevalent genetic alterations in the multistep process of malignant transformation [5–7]. However, it remains unclear whether telomere dysfunction induces chromosomal instability, initiating certain human epithelial malignancies. It has also recently been shown that DNA damage repair is activated early in most human epithelial carcinogenic processes [2, 3]. DNA damage repair mechanisms are thought to optimize cell survival after DNA damage, thereby controlling the proliferation of damaged cells. Two large, highly conserved protein kinases play a central role in the DNA damage response (DDR) mechanism in human cells: ataxia telangiectasia mutated (ATM) and ataxia telangiectasia related (ATR) kinases, which have different, but partly overlapping functions. Recent studies of human solid tumor samples obtained at different stages of carcinogenesis have revealed that activation of the DNA damage machinery is almost universal during the earliest stages of carcinogenesis [2, 3]. Early premalignant lesions (but not normal tissues) commonly express activated DDR markers. These markers include the phosphorylated kinases, ATM and Chk2, and p53. These findings are consistent with activation of an early ATR/ATM-regulated DDR network playing a role in

delaying or preventing cancer in human cells. Telomere attrition can result in short telomeres that the cell may detect as DNA damage. It has therefore been suggested that telomere attrition (together with oncogene activation) may lead to DNA damage checkpoint activation [1].

We evaluated telomere length and telomere protein levels and their relationship to DDR pathway activation in the multistep process of colorectal carcinogenesis. We studied colorectal carcinoma because this was the tumor type in which the multistep carcinogenesis model was first established. Tumor progression has been defined in detail in the colon, in which the earliest histological abnormalities are aberrant crypts with a focally atypical epithelium. These aberrant crypts may develop into benign epithelial tumors—low- and high-grade adenomas—which may in turn progress to malignant carcinoma. We evaluated telomere length, telomeric protein levels and DDR marker expression in consecutive tissue sections from matched patients presenting the major histological steps of colorectal carcinogenesis.

patients and methods

patients and tissue samples

Colon tissue samples were obtained from 15 patients, who underwent surgery at Assan Medical Center, Seoul, Republic of Korea. This series was unusual in that we had normal mucosal, low-graph dysplasia (LGD) and high-grade dysplasia (HGD) and invasive carcinoma (IC) samples from each individual patient. None of the patients had received radiotherapy or chemotherapy before surgery. After surgery, each tissue sample was fixed in formal and embedded in paraffin. Consecutive 4-μm thick paraffin tissue sections were mounted on polylysine-coated slides for analysis. Histological diagnoses were established by senior pathologists: SJJ, PN and EB. The Institute for Research in Biomedicine IRB of the Assan Medical Center, Seoul, Republic of Korea, decided that no ethical review of this study was necessary. Normal skin for antibody validation was obtained from a reductive mammoplasty as previously described [8].

antibodies

We used antibodies against Thr 68-phosphorylated Chk2 (#2661 Cell Signaling Technology, Danvers, MA) at a final dilution of 1/100, γ-H2AX (ser139) (#05-636 Upstate Biotechnology, Lake Placid, NY) at a final dilution of 1/200, Ser 1981-phosphorylated ATM (#200-301-500 Rockland Immunochemicals, Gilbertsville, PA) at a final dilution of 1/2500, TRF1 (#ab 10579-50, Abcam, Paris, France) at a final dilution of 1/100 and TRF2 (#05-521, Millipore, Paris, France) at a final dilution of 1/300.

cells and culture

We used HT-29 cells for antibody validation. HT-29 cells (obtained from LGC Promochem, Molsheim, France) were incubated in RPMI medium (Invitrogen, Carlsbad, CA) supplemented with 10% fetal bovine serum at 37°C, under an atmosphere containing 5% carbon dioxide. Cells were grown in 25-cm^2 flasks. For irradiation experiments, duplicate flasks of cells at 80% confluence were or were not subjected to irradiation with 3 Gy. The irradiated cells were incubated for 30 min at 37°C under an atmosphere containing 5% carbon dioxide treated with trypsin and harvested by centrifugation (800 *g*). They were then washed twice in cold phosphate-buffered saline (PBS) (#14190, Invitrogen). Cells were collected by centrifugation. The cell pellet was fixed by incubation in buffered formalin for 48 h and was then embedded in paraffin and cut into 4-μm sections with a microtome. These sections were mounted on polylysine-coated slides for analysis.

immunohistochemistry

Indirect immunoperoxidase staining was carried out on formalin-fixed tissue sections or cultured cells, using the Vectastain Elite kit (#PK-6200, Vector Laboratories, Burlingame, CA) or the Envision plus/horseradish peroxidase detection system (Dako, Carpinteria, CA).

Paraffin was removed from the sections, which were then rehydrated in a series of ethanol solutions with concentrations from 100% to 70%. Antigens were retrieved by heating (95°C) in 0.25 mM EDTA (pH 8) (for H2AX-p, ATM-p, Chk2-p) for 50 min or in Tris buffer (pH 6) (for TRF1, TRF2) for 60 min. Endogenous peroxidase activity was inhibited by immersing the slides in 3% hydrogen peroxide for 5 min. The slides were re-equilibrated with PBS and incubated with 1% normal horse serum or 2% bovine serum albumin, 0.02% normal goat serum and 0.01% Tween 20 for 20 min. Slides were incubated with primary antibody (diluted in 1% horse serum buffer) at room temperature for 2 h or overnight at 4°C. Slides were then incubated with either biotinylated secondary antibody followed by avidin–biotin peroxidase complex (PK-6200, Vector Laboratories) for 30 min each or a horseradish peroxidase-conjugated secondary antibody (K3468, Dako) for 30 min. A color reaction was developed using diaminobenzidine as the substrate. Slides were lightly counterstained with hematoxylin and mounted in permanent mounting medium.

The specificity of each antibody was assessed by western blotting before use to evaluate levels of the corresponding protein in irradiated and nonirradiated cells.

scoring of stained cells

Two investigators, including a senior pathologist, evaluated the immunostaining patterns independently. The percentage of positive tumor nuclei was calculated for each specimen, and a proportion score was assigned (0 if 0%, 0.1 if 1%–9%, 0.5 if 10%–49% and 1.0 if 50% or more). This proportion score was multiplied by the staining intensity of nuclei to obtain a final semiquantitative H score [9].

telomere length assessment by FISH

Telomere FISH was carried out as described by Meeker et al. [10]. Sections were deparaffinized and rehydrated antigens were then retrieved by heating for 15 min at 98°C in Tris buffer (pH 6). The sections were incubated with 0.1% Tween in PBS for 5 min, followed by 10% pepsin in 0.001 M HCl for 20 min at 37°C. Sections were then dehydrated and air dried. We applied 10 μl of a Cy3-labeled-specific peptide nucleic acid-targeting telomeres (Dako) to each sample, which was then covered with a coverslip and denatured by heating for 4 min at 83°C. Slides were placed in the dark for 2 h at 37°C to allow hybridization to occur. They were then washed twice for 15 min with formamide–Tris and three times, for 5 min each, in Tris–NaCl–Tween buffer at room temperature. They were counterstained with Diamidino-4′,6-phénylindol-2 dichlorhydrate (1 μg/ml) and mounted in aqueous mounting medium. The intensity of telomere staining, which is linearly related to telomere length, was assessed visually. Qualitative comparisons of staining were made between the epithelial regions of interest and adjacent epithelial cells of normal appearance or, if unavailable, normal adjacent stromal cells, such as lymphocytes, which invariably have robust telomere signals [6, 10, 11]. Nuclear telomeres were scored 0 (undetectable), 1 (intensity of fluorescent signal much less than for lymphocytes), 2 (signal intensity slightly lower than that for lymphocytes) or 3 (signal equivalent to that of normal epithelium or lymphocytes from the stroma).

statistical analysis

Tumor characteristics were compared using Fisher's exact test for categorical variables [the different histopathological stages: normal (N), LGD, HGD and IC] and pairwise Wilcoxon's test for continuous variables [p-ATM (Ser1981), p-Chk2 (Thr 68), γ-H2AX, TRF1 and TRF2

expressions]. A generalized linear model was used to assess correlations between continuous variables. Differences were considered significant if a two-sided P value <0.05 was obtained. All statistical analyses were carried out with SAS version 9.13 (SAS Institute Inc, Cary, NC).

results

antibody validation

Immunostaining was carried out on paraffin-embedded tissues and cultured cells to assess the specificity of staining with the various antibodies used. Normal human skin and human HT-29 colorectal cancer cells were evaluated at baseline and after exposure to radiation. Antibodies against H2AX phosphorylated at S139 (γ-H2AX), ATM phosphorylated at S1981 and Chk2 phosphorylated at T68 gave strong staining only with irradiated skin and colorectal cancer cells (Figure 1). γ-H2AX staining was punctate in irradiated colorectal cancer cells consistent with the development of foci. Staining was almost exclusively nuclear with the exception of weak cytoplasmic staining for ATM pS1981, which was not considered relevant in this study (Figure 1).

activation of the DDR

Normal colon tissues were only weakly stained for p-ATM, P-Chk2 and γ-H2AX. All three markers were significantly more strongly expressed in LGD (N versus LGD, P values: $P = 0.001$ for p-ATM, $P = 0.002$ for p-Chk2 and $P = 0.02$ for γ-H2AX) (Figure 2) (Table 1). There was also a trend for an increase in staining intensity for these markers between LGD and HGD, but this difference was not statistically significant. By contrast, the level of expression of these markers decreased between the HGD and invasive carcinoma stages ($P = 0.03$ for p-ATM, $P = 0.02$ for p-Chk2 and $P = 0.37$ for γ-H2AX) (Table 1). p-ATM levels were correlated with p-Chk2 levels ($P < 0.0001$, at all stages of carcinogenesis) but were only poorly correlated with γ-H2AX levels ($P = 0.065$ from normal tissue to HGD and $p = 0.067$ from HGD to invasive carcinoma) (Tables 2 and 3). γ-H2AX levels were correlated with p-Chk2 levels ($P = 0.0004$ from normal tissue to HGD and $P = 0.05$ from HGD to invasive carcinoma) (Tables 2 and 3). These observations suggest that the DNA damage repair pathway is already activated in LGD, this activation increasing in HGD, before being switched off in invasive tumors.

TRF1/2 expression

Strong TRF1 and TRF2 staining (level 3) was observed in normal colic tissue sections, particularly in basal epithelial cells. For TRF1 and TRF2, a net gradient of staining was observed in normal cells, from the base of the crypts (strong staining) to the lumen (weaker staining). TRF1 and TRF2 staining was weaker in LGD than in normal tissue (N versus LGD, P values = 0.004 for TRF1 and $P < 0.0001$ for TRF2) (Figures 3 and 4) (Table 1).

No significant difference in TRF1 and TRF2 staining was observed between LGD and HGD. However, staining for these two markers was stronger in invasive carcinoma

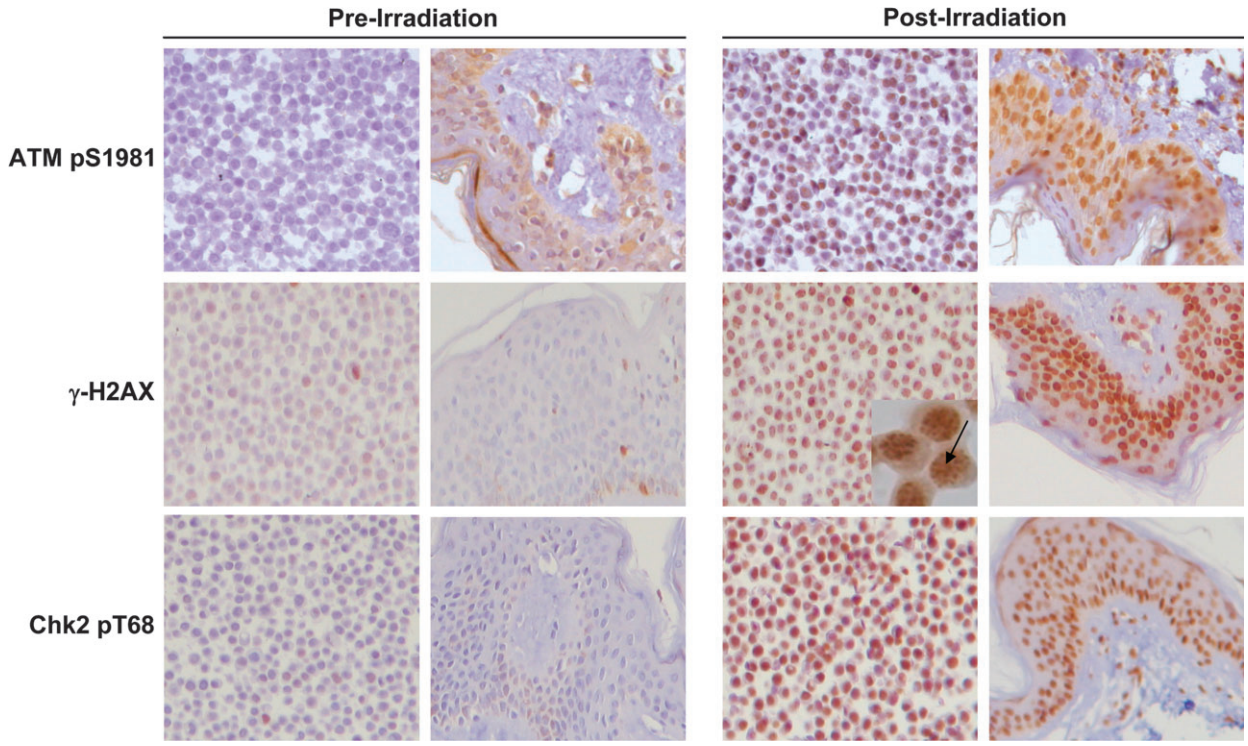

Figure 1. Normal human healthy skin and HT29 cells before and after *ex vivo* exposure to X-rays. Markers of an activated DNA damage response as detected by antibodies raised against ataxia telangiectasia-mutated pS1981, histone H2AX pS139 (γ-H2AX) and checkpoint kinase 2 pT68 become apparent in keratinocytes, stromal cells and cultured cells after irradiation. A magnification of histone H2AX pS139 (γ-H2AX) staining shows a staining in foci. Magnification ×400 of the samples are shown.

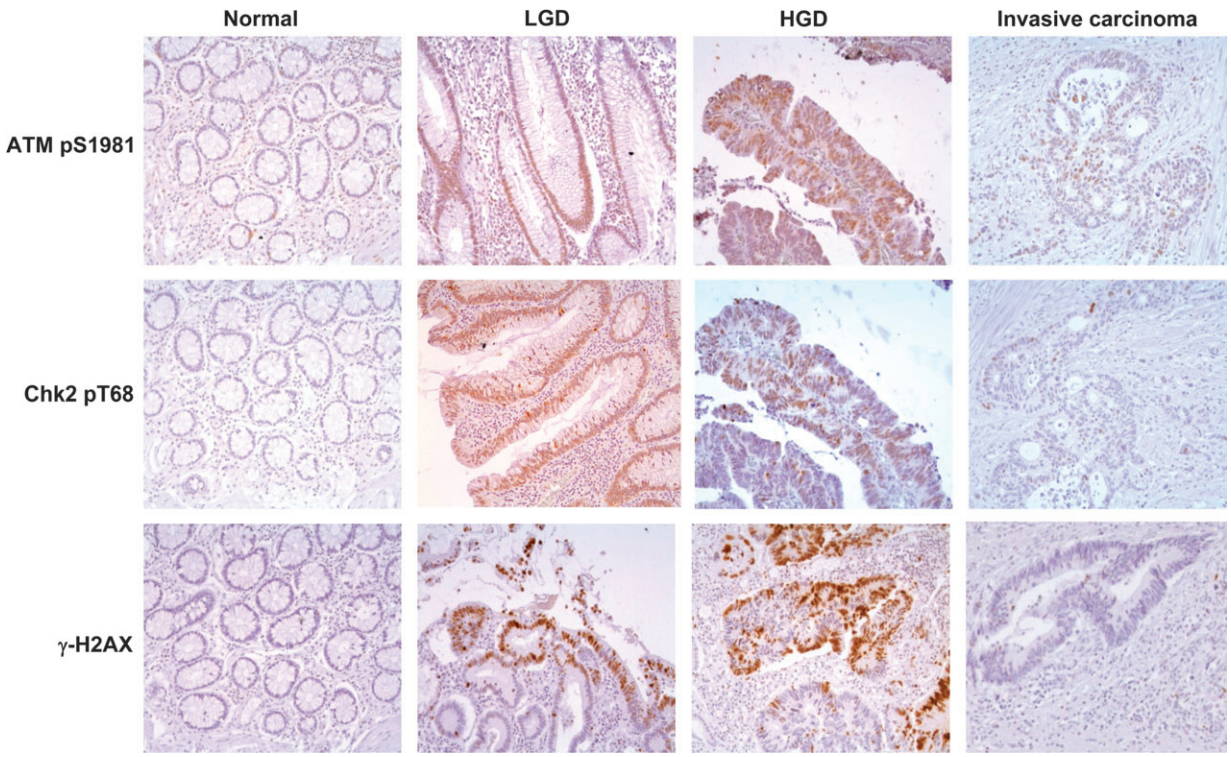

Figure 2. Representative images of colon-specific stages stained with ataxia telangiectasia-mutated pS1981, checkpoint kinase 2 pT68 and histone H2AX pS139 (γ-H2AX). Normal, low-grade dysplasia (LGD), high-grade dysplasia (HGD) and invasive carcinoma are shown. Note that no staining is displayed in normal crypts for any of the markers, a staining appear for each protein in LGD, an even more drastic staining in HGD and almost no more staining in invasive carcinoma. Magnification ×200 of the samples are shown.

Table 1. Statistical differences between stages for each protein

	ATM pS1981	CHK2 pT68	γ-H2AX	TRF1	TRF2	Telomere length
N versus LGD	0.001	0.002	0.02	0.004	<0.0001	<0.0001
N versus HGD	0.0005	0.0007	0.006	0.0005	<0.0001	<0.0001
LGD versus HGD	0.3	0.5	0.5	0.5	0.6	0.012
HGD versus invasive carcinoma	0.03	0.02	0.37	0.053	0.046	0.006

The table shows statistical differences between stages for each gene calculated with Wilcoxon test.
ATM, ataxia telangiectasia mutated; CHK2, checkpoint kinase 2; N, normal; LGD, low-grade dysplasia; HGD, high-grade dysplasia.

samples than in HGD samples ($P = 0.053$ and $P = 0.046$, for TRF1 and TRF2, respectively). We also found a significant correlation between TRF1 and TRF2 levels ($P < 0.0001$ from normal tissue to HGD and $P = 0.0014$ from HGD to invasive carcinoma) (Tables 2 and 3).

measurement of telomere length by telomere FISH

Histological analysis of telomere signals showed that telomere length depended on stage. The nuclei of normal basal epithelial cells and stromal lymphocytes contained a large number of fluorescent telomeric spots. These cells were assigned a score of 3. By contrast, LGD and, to an even greater extent, HGD cells were more weakly stained than internal controls. The decrease in staining with the transition from normal tissue to LGD and with that from LGD to HGD was statistically significant ($P < 0.0001$ and $P = 0.012$, respectively) (Figures 4 and 5; Table 1). During later stages of the carcinogenic process, staining increased with invasiveness, reaching the levels observed in normal cells in invasive carcinoma. This increase in staining associated with the transition from HGD to IC was also statistically significant ($P = 0.006$). The weakest telomeric signals were those obtained for HGD lesions. Moreover, as shown above, TRF1 and TRF2 levels were significantly correlated both with each other and with telomere lengthening during carcinogenesis ($P < 0.0001$ and $P < 0.0001$ for TRF1 and TRF2, respectively, for the transition from N to HGD and $P = 0.0104$ and $P = 0.0004$ for the transition from HGD to IC; Tables 2 and 3).

Table 2. Statistical correlation during the progression from N to HGD

N versus HGD	CHK2 pT68	γ-H2AX	TRF1	TRF2	Telomere length
ATM pS1981	<0.0001	0.065	0.0005	0.0003	<0.0001
CHK2 pT68		0.0004	0.11	0.0096	0.0005
γ-H2AX			0.042	0.010	0.002
TRF1				<0.0001	<0.0001
TRF2					<0.0001

Correlation values between DNA damage response protein activation, TRF1 and TRF2 expressions and telomere length during the progression from N to HGD.
N, normal; ATM, ataxia telangiectasia mutated; CHK2, checkpoint kinase 2; HGD, high-grade dysplasia.

Table 3. Statistical correlation during the progression from HGD to invasive carcinoma

HGD versus invasive carcinoma	CHK2 pT68	γ-H2AX	TRF1	TRF2	Telomere length
ATM pS1981	<0.0001	0.067	0.5406	0.1807	0.1737
CHK2 pT68		0.05	0.2026	0.0154	0.1883
γ-H2AX			0.0927	0.2063	0.1564
TRF1				0.0014	0.0104
TRF2					0.0004

Correlation values between DNA damage response protein activation, TRF1 and TRF2 expressions and telomere length during the progression from HGD to invasive carcinoma.
HGD, high-grade dysplasia; ATM, ataxia telangiectasia mutated; CHK2, checkpoint kinase 2.

discussion

Consistent with published data [6, 8, 12, 13], our results show that telomere attrition occurs early in carcinogenic progression in the colon model, with telomere shortening observed in LGD. This attrition peaks in HGD, and it is only when the full invasive potential of the tumor has been reached that telomere length returns to levels close to those observed in normal tissue. We hypothesize that this telomere attrition may have a protective effect against cancer because critically short telomeres are known to induce a cell cycle arrest commonly known as replicative senescence.

We also demonstrate for the first time that levels of the two major telomere-associated proteins—TRF1 and TRF2—are correlated, both with each other and with telomere length during colon carcinogenesis. This finding is consistent with the partially overlapping roles of TRF1/2. The loss of TRF1 and TRF2 accompanied by telomere shortening in LGD and HGD provides support for the notion that telomere attrition occurs *in vivo* and may disturb telomeric homeostasis.

We also observed signs of DDR activation, including the phosphorylation of H2AX, Chk2 and ATM, during colorectal carcinogenesis. This DDR activation, which is barely detectable in normal crypts, is induced at some point during the transition from normal tissue to LGD. The DDR was maximal in HGD. By contrast, only low levels of DDR activation were observed in fully invasive cells, suggesting that neoplastic cells may have avoided apoptosis by impairing DDR.

Both telomere length and TRF1/2 levels were inversely correlated with DDR activation. There are three possible explanations for this inverse correlation: (i) DDR may be oncogene induced and related to DNA replication stress [2]. In this case, telomere attrition would be the consequence of unregulated cell proliferation. (ii) Telomeres may play an indirect role in DDR activation. Indeed, once they reach a critical size, telomeres lose their normal three-dimensional

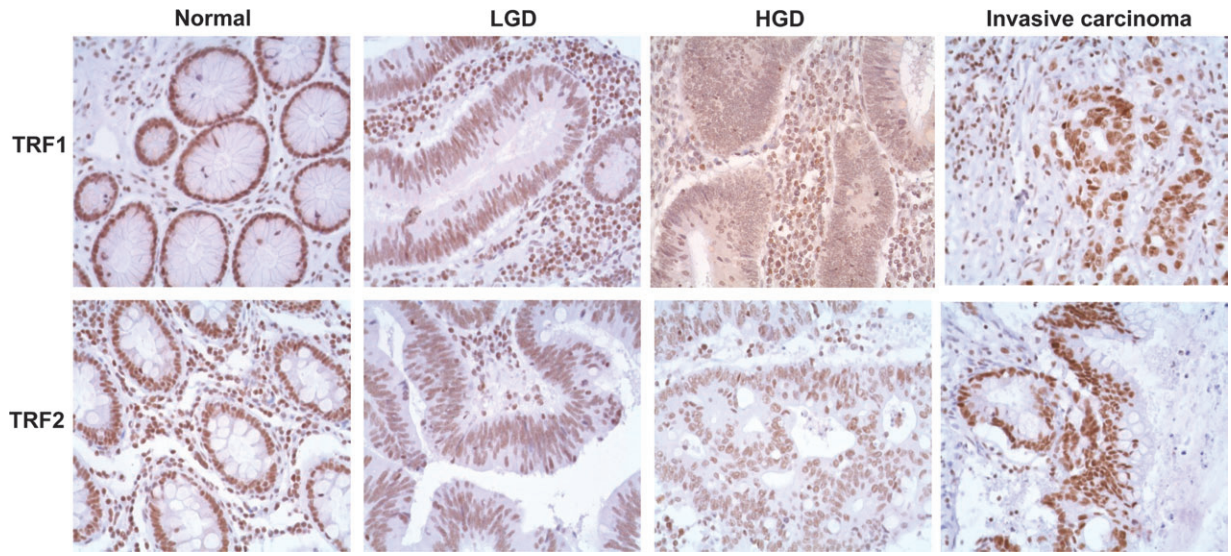

Figure 3. Representative images of colon-specific stages stained with TRF1 and TRF2. Normal, low-grade dysplasia (LGD), high-grade dysplasia (HGD) and invasive carcinoma are shown. Note that a strong staining comparable to stromal cells are displayed in normal crypts, the same staining is lower in LGD and even weaker in HGD and very strong staining is observed in invasive carcinoma. Magnification ×400 of the sample are shown.

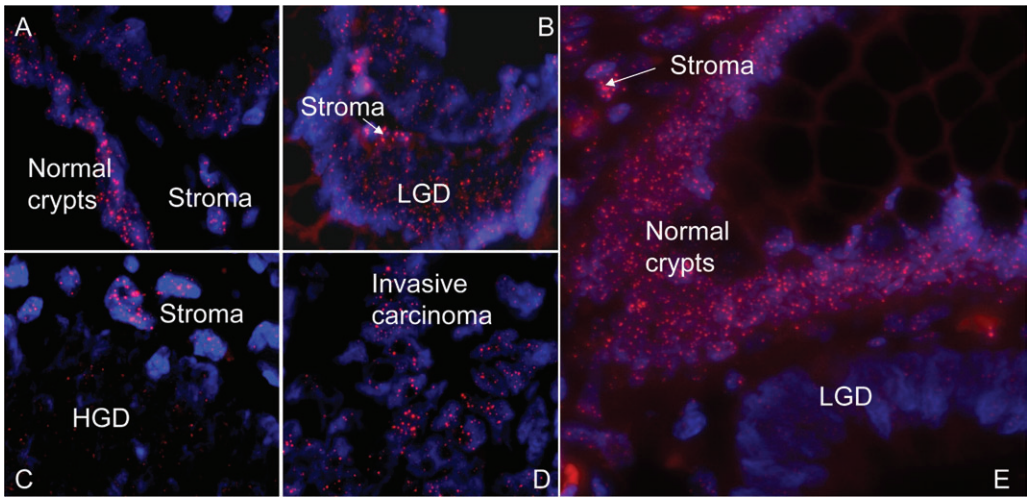

Figure 4. Telomere length along carcinogenesis. Telomere length abnormalities in intraepithelial neoplasia lesions of the large intestine. Representative images of normal, low-grade dysplasia (LGD), high-grade dysplasia (HGD) and colic invasive carcinoma stained for telomeric DNA (red, Cy3-labeled anti-telomeric peptide nucleic acid probe) and total DNA (blue, 4,6-diamidino-2-phenylindole stain). The fluorescence intensity of the telomeric signals is linearly related to telomeric DNA length. (A) Normal colic crypt show robust telomere staining comparable with surrounding stromal cells (S). (B) Note decreased telomeric signal in LGD compared with stromal cells. (C) Drastic loss of telomere signal in HGD in comparison to stromal cells. (D) Invasive carcinoma show robust telomere staining comparable with normal level or stromal cells. (E) Adjoining areas of adenomatous and normal colonic epithelia. Note the drastic loss of telomeric signal in LGD in comparison to the normal counterpart.

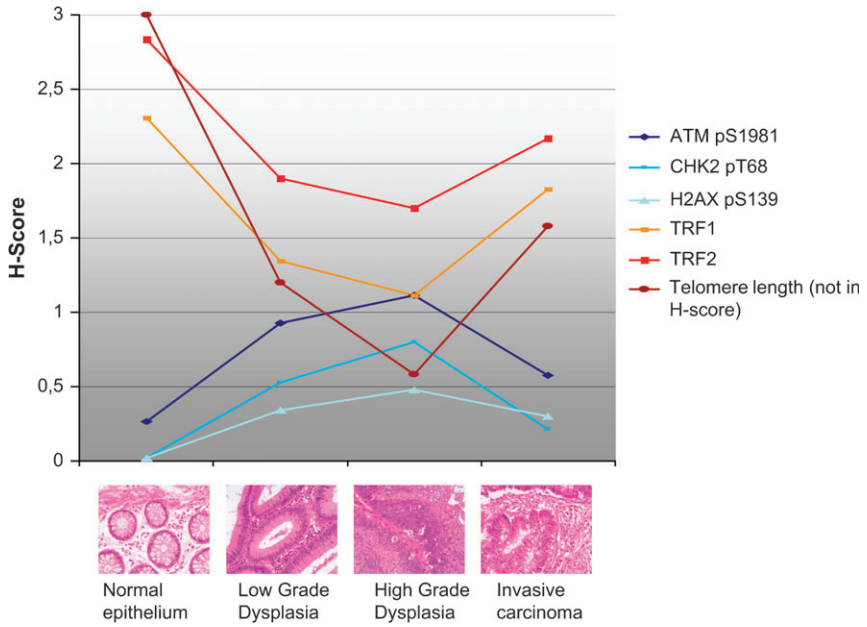

Figure 5. DNA damage response (DDR), TRF1/2 expression and telomere length in colon carcinogenesis. H score is shown on the vertical axis. The horizontal axis describes the stage of the lesion. DDR proteins are shown to be almost nonactivated in normal crypts but activated in low-grade dysplasia (LGD) and more drastically in high-grade dysplasia (HGD); finally they are deactivated in invasive lesions. In contrast, TRF1/2 that are strongly expressed in the normal layers are down-regulated in LGD and HGD and reexpressed in invasive lesions.

(3-D) structure. This may result in telomeric fusions and subsequent break fusion bridge cycles. These events may lead to general genomic instability, activating the DDR. (iii) The DDR may be directly activated by telomeres that are too short. Indeed, it has been shown that very short telomeres are associated with telomeric epigenetic modifications and H2AX phosphorylation at telomeres leading to DDR activation [1, 14]. This hypothesis is consistent with the decrease in TRF1/2 levels accompanying telomere attrition. Indeed, previous studies have demonstrated that TRF2 has ATM dephosphorylation activity [15–17]. Thus, following the 3-D stabilization of telomeres, which is thought to protect the ends of the chromosomes from DNA damage sensors, TRF2 may be directly involved in ensuring that telomeres are not recognized as double strand breaks (DSBs). In this case, once cells go beyond replicative senescence, their telomeres would be too

short to be protected and would therefore be recognized as DSBs. However, demonstrations of the colocalization of short telomeres and γ-H2AX on the same tissue sample are required to confirm this hypothesis. Such a demonstration would be very difficult technically. Telomere visualization on paraffin tissue sections generally requires a protease treatment of slides, leading to the partial or complete destruction of γ-H2AX foci and problems identifying the remaining observable foci as such. Moreover, under this hypothesis, only the shortest telomeres would be recognized as DSBs and carry H2AX foci, and isolated short telomeres are extremely difficult to visualize in human paraffin tissue sections. It might be simpler to work on fresh tissues or frozen material, but this would make it difficult to obtain a cohort of this type, with samples from LGD to invasive carcinoma for the same patients.

A recent study [8] has shown that DDR activation may be tissue specific. By contrast to our observations and those of other groups [18–20], TRF1 and TRF2 have been shown to be overproduced in neoplastic lung lesions [21]. It would therefore be of great interest to determine whether the telomere/DDR activation correlation observed here depends on histological type. Analyses of lung, prostate and breast tissues (together with colon, corresponding to the four most common cancers worldwide), in particular, would be of great value.

Several drugs that target the telomeres and their related proteins are tested in preclinical models and in early clinical trials these days, and one of the suggested mechanisms of action is the induction of progressive telomere shortening and a direct damage of the structure of individual telomeres [22, 23]. While their clinical impact has not been yet demonstrated in patients with an invasive disease, some *in vivo* models have shown that a pretreatment of tumor cells with such inhibitors led to a marked reduction in their tumorigenic potential [22]. Our demonstration that telomere shortening occurs in LGD and HGD raises the hypothesis that telomere interacting agents could have a role not only at the time of invasive disease but also earlier in the carcinogenic progression of colon cancer, favoring the telomere attrition and the activation of apoptosis in the dysplastic cell. In fact, this approach of reversion of premalignant lesions has already been tested with other targeted molecules in *in vivo* lung cancer multistep models [24, 25].

funding

TELINCA and RISC-RAD (FI6R-CT2003-508842). Christophe Raynaud is a doctoral fellow funded by a CEA-Lilly fellowship.

acknowledgements

The work carried out in the L.S. laboratory. We would like to thank Dr Fabrizio D'adda di Fagagna for helpful discussions and exchanges.

references

1. d'Adda di Fagagna F, Reaper PM, Clay-Farrace L et al. A DNA damage checkpoint response in telomere-initiated senescence. Nature 2003; 426: 194–198.
2. Bartkova J, Horejsi Z, Koed K et al. DNA damage response as a candidate anti-cancer barrier in early human tumorigenesis. Nature 2005; 434: 864–870.
3. Gorgoulis VG, Vassiliou LV, Karakaidos P et al. Activation of the DNA damage checkpoint and genomic instability in human precancerous lesions. Nature 2005; 434: 907–913.
4. Greider CW, Blackburn EH. A telomeric sequence in the RNA of Tetrahymena telomerase required for telomere repeat synthesis. Nature 1989; 337: 331–337.
5. Meeker AK, Hicks JL, Gabrielson E et al. Telomere shortening occurs in subsets of normal breast epithelium as well as in situ and invasive carcinoma. Am J Pathol 2004; 164: 925–935.
6. Meeker AK, Hicks JL, Iacobuzio-Donahue CA et al. Telomere length abnormalities occur early in the initiation of epithelial carcinogenesis. Clin Cancer Res 2004; 10: 3317–3326.
7. Meeker AK, Hicks JL, Platz EA et al. Telomere shortening is an early somatic DNA alteration in human prostate tumorigenesis. Cancer Res 2002; 62: 6405–6409.
8. Nuciforo PG, Luise C, Capra M et al. Complex engagement of DNA damage response pathways in human cancer and in lung tumor progression. Carcinogenesis 2007; 28: 2082–2088.
9. Olaussen KA, Dunant A, Fouret P et al. DNA repair by ERCC1 in non-small-cell lung cancer and cisplatin-based adjuvant chemotherapy. N Engl J Med 2006; 355: 983–991.
10. Meeker AK, Gage WR, Hicks JL et al. Telomere length assessment in human archival tissues: combined telomere fluorescence in situ hybridization and immunostaining. Am J Pathol 2002; 160: 1259–1268.
11. Lansdorp PM, Verwoerd NP, van de Rijke FM et al. Heterogeneity in telomere length of human chromosomes. Hum Mol Genet 1996; 5: 685–691.
12. Engelhardt M, Drullinsky P, Guillem J, Moore MA. Telomerase and telomere length in the development and progression of premalignant lesions to colorectal cancer. Clin Cancer Res 1997; 3: 1931–1941.
13. Garcia-Aranda C, de Juan C, Diaz-Lopez A et al. Correlations of telomere length, telomerase activity, and telomeric-repeat binding factor 1 expression in colorectal carcinoma. Cancer 2006; 106: 541–551.
14. d'Adda di Fagagna F, Teo SH, Jackson SP. Functional links between telomeres and proteins of the DNA-damage response. Genes Dev 2004; 18: 1781–1799.
15. Celli GB, de Lange T. DNA processing is not required for ATM-mediated telomere damage response after TRF2 deletion. Nat Cell Biol 2005; 7: 712–718.
16. Karlseder J, Broccoli D, Dai Y et al. p53- and ATM-dependent apoptosis induced by telomeres lacking TRF2. Science 1999; 283: 1321–1325.
17. Karlseder J, Hoke K, Mirzoeva OK et al. The telomeric protein TRF2 binds the ATM kinase and can inhibit the ATM-dependent DNA damage response. PLoS Biol 2004; 2: E240.
18. Kishi S, Wulf G, Nakamura M, Lu KP. Telomeric protein Pin2/TRF1 induces mitotic entry and apoptosis in cells with short telomeres and is down-regulated in human breast tumors. Oncogene 2001; 20: 1497–1508.
19. Yamada M, Tsuji N, Nakamura M et al. Down-regulation of TRF1, TRF2 and TIN2 genes is important to maintain telomeric DNA for gastric cancers. Anticancer Res 2002; 22: 3303–3307.
20. Miyachi K, Fujita M, Tanaka N et al. Correlation between telomerase activity and telomeric-repeat binding factors in gastric cancer. J Exp Clin Cancer Res 2002; 21: 269–275.
21. Nakanishi K, Kawai T, Kumaki F et al. Expression of mRNAs for telomeric repeat binding factor (TRF)-1 and TRF2 in atypical adenomatous hyperplasia and adenocarcinoma of the lung. Clin Cancer Res 2003; 9: 1105–1111.
22. Damm K, Hemmann U, Garin-Chesa P et al. A highly selective telomerase inhibitor limiting human cancer cell proliferation. EMBO J 2001; 20: 6958–6968.
23. El-Daly H, Kull M, Zimmermann S et al. Selective cytotoxicity and telomere damage in leukemia cells using the telomerase inhibitor BIBR1532. Blood 2005; 105: 1742–1749.
24. Wislez M, Spencer ML, Izzo JG et al. Inhibition of mammalian target of rapamycin reverses alveolar epithelial neoplasia induced by oncogenic K-ras. Cancer Res 2005; 65: 3226–3235.
25. Yang Y, Wislez M, Fujimoto N et al. A selective small molecule inhibitor of c-Met, PHA-665752, reverses lung premalignancy induced by mutant K-ras. Mol Cancer Ther 2008; 7: 952–960.